

Spin and Orbital Magnetic Moments of Free Nanoparticles

S. Peredkov,¹ M. Neeb,² W. Eberhardt,¹ J. Meyer,³ M. Tombers,³ H. Kampschulte,³ and G. Niedner-Schatteburg³

¹*Institut für Optik und Atomare Physik, Technische Universität Berlin, Hardenbergstrasse 36, 10623 Berlin, Germany*

²*Helmholtz-Zentrum Berlin für Materialien und Energie, BESSY II, Albert-Einstein-Strasse 15, 12489 Berlin, Germany*

³*Fachbereich Chemie und Forschungszentrum OPTIMAS, TU Kaiserslautern, 67663 Kaiserslautern, Germany*

(Received 27 June 2011; published 30 November 2011)

The determination of spin and orbital magnetic moments from the free atom to the bulk phase is an intriguing challenge for nanoscience, in particular, since most magnetic recording materials are based on nanostructures. We present temperature-dependent x-ray magnetic circular dichroism measurements of free Co clusters ($N = 8\text{--}22$) from which the *intrinsic* spin and orbital magnetic moments of non-interacting magnetic nanoparticles have been deduced. An exceptionally strong enhancement of the orbital moment is verified for free magnetic clusters which is 4–6 times larger than the bulk value. Our temperature-dependent measurements reveal that the spin orientation along the external magnetic field is nearly saturated at ~ 20 K and 7 T, while the orbital orientation is clearly not.

DOI: 10.1103/PhysRevLett.107.233401

PACS numbers: 36.40.Cg, 33.15.Kr, 78.70.Dm

Free transition metal atoms possess large spin and orbital magnetic moments according to Hund's rules. Bulk formation, on the other hand, causes a substantial attenuation of the spin (m_S) and orbital (m_L) moments. The latter can even be completely quenched in macroscopic systems, as shown by x-ray magnetic circular dichroism (XMCD) measurements on ferromagnetic bulk samples [1,2]. Thus, one of the main concerns of magnetism is to understand how magnetic properties change when going from the electronic structure of a single atom to the bulk, i.e., when orbital hybridization, geometry, symmetry breaking, electron delocalization, and band formation come into play. Mass-selected clusters are most suitable objects to follow the evolution of magnetism as a function of size. Total magnetic moments (m_{tot}) of free mass-selected clusters have been determined by ingenious Stern-Gerlach experiments [3–5]. However, spin and orbital magnetic moments of free magnetic particles like molecular magnets and clusters are experimentally unknown due to a lack of magnetosensitive experiments for probing an extremely dilute target density of some attomoles/cm³. Since the orbital moments are influenced more strongly by orbital hybridization and electron delocalization, it is important to quantify them and to study their size and temperature dependence. Do m_S and m_L reveal the same size dependence, or do they vary independently? On which length scale does the orbital momentum get quenched, and when does the spin moment converge to the bulk value? Is there a monotonic size evolution, or do m_S and m_L exhibit a non-scalable size dependence? Do m_S and m_L exhibit the same temperature dependence? Considerable efforts have been invested for the calculation of spin and orbital magnetic moments of free clusters which still await experimental data for comparison and code refinement [6–8]. Large orbital moments are expected to cause a large magnetic anisotropy and thus might play a crucial role in the inherent

orientation of magnetic moments along a preferred spatial coordinate of the cluster, an important prerequisite for being used as magnetic data storage material.

Atomic islands, wires, and nanoparticles as well as supported clusters have been explored by XMCD in order to determine size-dependent information and to study the dependence of magnetic moments and anisotropy on dimensionality [9–14]. Common to all these measurements is that the explored particles are in contact with a support material. Extrinsic effects on the magnetic properties are inevitably due to modifications of geometry, electronic structure, charge transfer, and hybridization with the support. Thus, the determination of the intrinsic moments of free magnetic particles is extremely important for both experiment and theory, as the data elucidate the influence of the support on the magnetic properties of application-relevant deposited clusters and, on the other hand, as the measured moments can be used as reference data for highly sophisticated calculations.

Here we present XMCD data on free “ferromagnetic” nanoparticles which have been used to extract the intrinsic spin and orbital magnetic moments of small Co_N cluster ions as a function of the number of atoms $N = 8\text{--}22$. Note that Co_N clusters are expected to possess orbital moments that are higher than those of other itinerant ferromagnetic elements like Fe and Ni [7]. The total magnetic moment m_{tot} , which is given by the vector sum of m_S and m_L , is compared with the magnetic moments as obtained from prior Stern-Gerlach experiments [5,15,16]. Interestingly, our data are systematically higher than those of Refs. [5,15] but are close to the magnetic moments of Ref. [16]. We might be able to solve this apparent mismatch by using the different temperature dependence of spin and orbital moments as will be explained in the following.

In order to record XMCD spectra of free mass-selected clusters, a Fourier transform ion cyclotron resonance mass

spectrometer has been combined with a soft-x-ray synchrotron beam line at BESSY. The experimental setup has been described in detail in Ref. [17] and Fig. S1 [18]. Figure 1(a) shows L -edge absorption curves of Co_{12}^+ which have been taken at a buffer-gas equilibrated cluster temperature of 20 K using right- and left-handed circular polarization of the x-ray light. The L_3 and L_2 edges are clearly resolved. The XMCD signal ($\sigma^+ - \sigma^-$) at the L_3 edge is very prominent, while it is much smaller at the L_2 edge [Fig. 1(b)].

Magneto-optical sum rules [19–21] have been used to extract the measured projection of the spin and orbital magnetic moments $m_S^{(z)}$ and $m_L^{(z)}$ [22]. The quantization axis z is defined by the direction of the applied magnetic trapping field. For a quantitative determination of spin and orbital magnetic moments, we used Eqs. (1) and (2) of the paper of Chen *et al.* [21]. Rewriting the formula of Ref. [21] by replacing A and B for the corresponding integrated XMCD signal $\int(\sigma^+ - \sigma^-)$ of the L_3 and L_2 edge, respectively, and C for the integral of the sum of the two helicity-dependent absorption curves $\int(\sigma^+ + \sigma^-)$, we obtain

$$m_L^{(z)} = -\frac{4(A+B)}{3C}n_h, \quad (1)$$

$$m_S^{(z)} = -\frac{2(A-2B)}{C}n_h - 7T_z. \quad (2)$$

$m_L^{(z)}$ and $m_S^{(z)}$ are given per atom in units of μ_B ; n_h represents the number of $3d$ holes which has been set equal to the bulk value, $n_h = 2.5$ [21]. We use the bulk value instead of the atomic value ($n_h = 3$) in order to take an intra-atomic charge redistribution $4s \rightarrow 3d$ into account. This enables bonding between two adjacent Co atoms [23], as otherwise the $4s\sigma_g$ bond is compensated by an antibonding $4s\sigma_u$ orbital. $\langle T_z \rangle$ corresponds to the expectation value of the spin magnetic dipole operator for the spin quantization axis oriented along z [21,24], which defines the asymmetry of the intra-atomic spin distribution. It is nonzero in anisotropic bonding environments due to the different number of spins in the unit cell along different crystallographic directions, but it vanishes when an angular average is performed [25,26]. According to theory, the absolute value of $7T_z$ for systems with low dimensionality such as surfaces and deposited clusters can range up to 20% of the spin magnetic moment [24,27]. In our study we are dealing with freely rotating particles which are not fixed in space. As T_z is a strongly directional value, we have good reasons to assume that T_z , which can adopt values of different sign, averages to a minimum value close to zero.

Applying the above sum rules, the analysis reveals that the measured orbital moments $m_L^{(z)}$ at 20 K and $B = 7$ T are clearly enhanced (2–4 times) with respect to the bulk [21], while the measured spin moments $m_S^{(z)}$ of the clusters

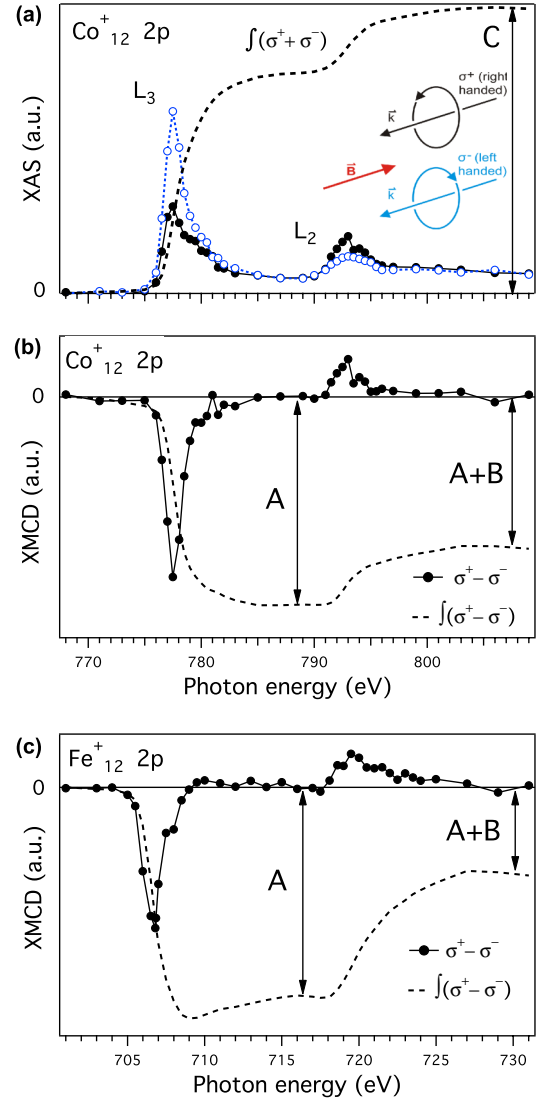


FIG. 1 (color online). (a) Circularly polarized x-ray absorption spectra of Co_{12}^+ at the L edge. The spectrum recorded with negative polarization (σ^-) is shown by open circles and a dotted line (blue), that with positive polarization (σ^+) by filled dots and a full line (black). The relative orientation of polarization, light propagation (k), and magnetic field (B) is shown in the cartoon. The integration of the sum of both absorption curves is shown as a dashed line (C), which is used for calculation of the magnetic moments according to the magneto-optical sum rules. (b) The XMCD spectrum ($\sigma^+ - \sigma^-$) of Co_{12}^+ after subtracting the L -edge-jump intensity. A and B correspond to the area of the L_3 and L_2 dichroic intensity, respectively. The integration of the dichroic intensity is shown as a dashed line ($A+B$). Note that the large absolute value of ($A+B$) exhibits a strong orbital moment. (c) L -edge XMCD spectrum of Fe_{12}^+ measured under the same conditions.

($N = 8$ – 22) are less strongly enhanced (< 1.4 times) as summarized in Table S2 [18].

Figure 1(c) exemplarily demonstrates that the enhancement of the orbital moment is not just seen for Co clusters

but also for small Fe clusters [28]. The XMCD signal ($A + B$) is clearly larger than that of bulk iron, which almost vanishes [21]. The measured orbital moment $m_L^{(z)}$ amounts to $0.25 \mu_B/\text{atom}$ compared to the bulk value of $0.085 \mu_B/\text{atom}$ [21].

According to the classical Langevin equation, which applies for single domain particles, the magnetization of small magnetic particles is expected to scale inversely with the temperature at a given B field [29–31]. Indeed, the measured moments $m_{L,S}^{(z)}$ show a striking temperature dependence as typical for superparamagnetic particles (Fig. 2). Our 7 T strong magnetic field substantially exceeds the Paschen-Back limit for atoms ~ 1 T, and therefore orbital and spin angular momentum can be expected to decouple. This can be quantitatively rationalized by the relatively weak spin-orbit interaction energy of the itinerant $3d$ metals. The magnetic energy of Co_{11}^+ is 1–2 meV/atom at a field strength of 7 T. This energy compares with the spin-orbit splitting of a few meV for the bulk as well as the magnetic anisotropy energy as calculated for the atoms of a Co monolayer [32,33]. Based on these estimates and our observation of a change in the ratio $m_L^{(z)}/m_S^{(z)}$ with temperature, we apply the classical Langevin equation to fit the temperature dependence of spin and orbital moments separately. According to the Langevin function, the intrinsic magnetic orbital and spin moments m_L and m_S per atom in units of μ_B are given by

$$m_{L,S}^{(z)}(T) = m_{L,S} \left[\coth\left(\frac{Nm_{L,S}\mu_B B}{k_B T}\right) - \frac{k_B T}{Nm_{L,S}\mu_B B} \right]. \quad (3)$$

$m_{L,S}^{(z)}(T)$ are the temperature-dependent projected orbital and spin magnetic moments per atom in units of μ_B and N denotes the number of atoms in the cluster. As shown in Fig. 2, a least-squares fit has been used to fit the data $m_L^{(z)}(T)$ and $m_S^{(z)}(T)$ with the above Langevin functions

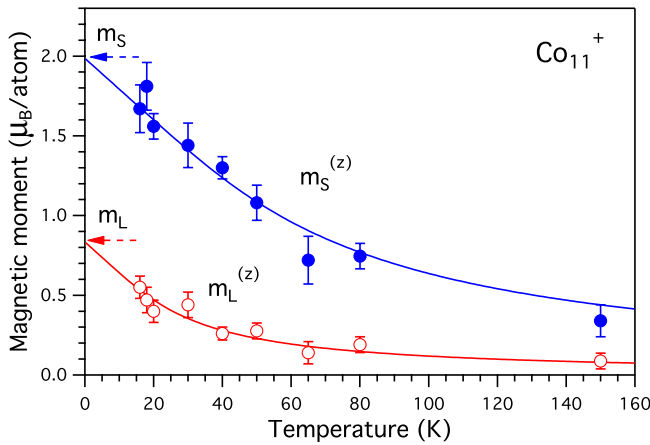


FIG. 2 (color online). Measured spin and orbital magnetic moment ($m_{L,S}^{(z)}$) versus temperature of Co_{11}^+ . The line through the measured moments is a Langevin fit using $B = 7$ T.

using the intrinsic moments m_S and m_L as fitting parameters. No hints for freezing of the magnetization into a blocked state is observed down to 20 K in agreement with measurements on Co wires [9]. Moreover, Fig. 2 clearly shows that at 20 K the spin moment is much closer to its saturation limit than the smaller orbital moment. It is obvious that lower temperatures are necessary to saturate the orbital moment due to its smaller magnetic energy. In other words, the alignment of the orbital moment along the external field is weaker than the alignment of the larger spin moment. From this we conclude that spin and orbital moments are decoupled and interact separately with the external field analogous to the Paschen-Back effect in atoms [34].

Upon scaling $m_L^{(z)}(T)$ and $m_S^{(z)}(T)$ to the saturation limit at $T = 0$ K, the measured moments $m_{L,S}^{(z)}(T = 20 \text{ K})$ need to be corrected by $\sim 15\%$ and $\sim 70\%$, respectively, to determine the intrinsic moments m_S and m_L . The corrections become larger the smaller the moments are, as the alignment along the magnetic field direction is thermally less stable. The Langevin-scaled intrinsic spin and orbital moments of the Co_N clusters are plotted in Fig. 3. The moments develop in a nonscalable manner from one cluster size to the next. Seemingly, the spin moment fluctuates more with cluster size N than the orbital moment. A convergence towards the bulk magnetic moments is not obvious up to clusters containing 22 atoms. The intrinsic spin moments of the clusters are in the range $m_S = 2\text{--}2.7 \mu_B$ per atom, while the orbital moments amount to $m_L = 0.6\text{--}1 \mu_B$ per atom. Thus the intrinsic orbital

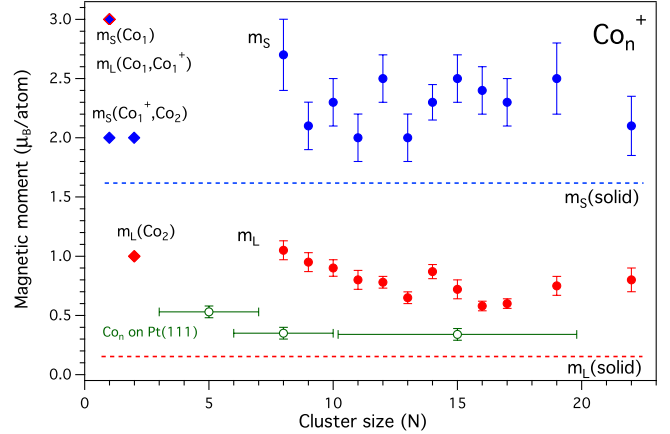


FIG. 3 (color online). Magnetic moments as revealed from XMCD spectra using magneto-optical sum rule analysis. Filled symbols show the intrinsic spin (m_S , blue) and orbital magnetic moments (m_L , red) of the clusters after Langevin scaling of the measured moments ($m_S^{(z)}$, $m_L^{(z)}$) recorded at 20 K and 7 T. The error bar corresponds to the standard deviation ($\pm 2\sigma$) from repeated measurements at 778 eV (cf. Fig. S1 [18]). Moments of Co bulk [21] (dotted line) and small atomic islands [35] (green full line) are indicated. Additionally, the corresponding moments of the atom (Co_1 ^4F ; Co_1 ^{+3}F) and dimer (Co_2 $^5\Delta$) are displayed.

moments of the clusters are 4–6 times larger than the value of the solid, and the spin moments are enhanced by a factor of 1–2. Also, the intrinsic orbital moments of free clusters are enlarged with respect to small atomic islands formed on a crystalline platinum surface [35] as shown in Fig. 3.

The intrinsic orbital moment of a pentagonal bipyramid with a d -band filling of 2.5 (Co_7) has been calculated to be $0.7 \mu_B/\text{atom}$ for magnetization along the equatorial C_2 axis [6] which comes close to our measured orbital moments. The orbital moment of the dimer $m_L = 1 \mu_B/\text{atom}$, as approximated from Hund's rule for the ground state configuration $^5\Delta$ [23,36–38], is also similar to m_L of the clusters. However, the orbital moment of the atom (4F [37], $m_L = 3\mu_B$) is distinctly larger, which suggests a sudden drop of m_L from the atom to the dimer. Towards larger clusters, m_L further diminishes but rather smoothly. The moment of Co_{13}^+ represents a local minimum which might hint at a highly symmetric structure (I_h) of this cluster. The intrinsic spin moments of the clusters are somewhat higher than the calculated ones, which are in the range $m_S = 1.9\text{--}2.1 \mu_B/\text{atom}$ for $\text{Co}_{2\text{--}20}$ [8], while they are smaller than this of the neutral atom ($3\mu_B$) [39]. Moreover, the XMCD measurements show that the ratio m_L/m_S of the clusters, which is independent of n_h , is 3–4 times higher than that of the solid ($m_L/m_S = 0.1$).

In Fig. 4, we compare the total magnetic moments $m_{\text{tot}} = m_S + m_L$ as revealed from our XMCD measurements with the results from earlier Stern-Gerlach

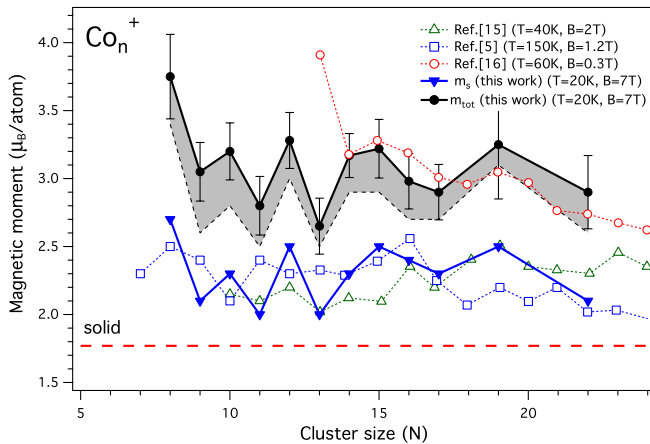


FIG. 4 (color online). Total magnetic moments of Co_N^+ clusters as determined by XMCD (filled dots) in comparison with Stern-Gerlach results (open symbols) taken from Ref. [5,15,16]. The spin moments as revealed from XMCD are also shown (filled triangles). [The transition from fully coupled to decoupled moments changes gradually with the strength of the magnetic field. This affects the Langevin scaling of the measured moments which is indicated by the shaded region of the total moment. The boundaries for total coupling and decoupling are shown by the lower line (dotted) and upper line (bold). The intrinsic orbital moment (not shown) drops by 30%–40% when coupled moments are considered while the spin moment hardly ever changes.]

experiments [5,15,16]. In these earlier experiments, the spatial deflection of neutral clusters in an inhomogeneous magnetic field is used as a measure of the total magnetic moment of the clusters. As the Stern-Gerlach data are analyzed by the Langevin model [5,15,16], the published data can directly be compared to the sum of our scaled moments. Two of the Stern-Gerlach series [5,15] show very similar results with magnetic moments ranging between 2 and $2.5\mu_B$ per atom, while another series exhibits much higher moments between 3 and $4\mu_B$ per atom [16]. Remarkably, the lower Stern-Gerlach data agree with the measured spin moments rather than with the sum of the spin and orbital moment. We therefore conclude that the magnetic moments of Refs. [5,15] represent basically the spin moment, while the contribution of the orbital magnetic moment is relatively reduced. This might be explained as follows: The data of Xu *et al.* [15] and Knickelbein [5] have been measured with a magnetic field of 1.2 and 2 T, respectively. It is likely that under these field strengths spin and orbital moments interact rather independently with the external B field similar to our experiment. As established by our temperature-dependent measurements (Fig. 2), the orbital moment is less aligned along the magnetic field direction than the larger spin moment. For example, the orbital contribution $m_L^{(c)}$ to the measured total magnetic moment is less than 15% at 1 T and 40 K. The individual temperature dependence of spin and orbital moments must be compensated for by different scaling factors in order to deduce the intrinsic moments. Note that the weaker orbital moment must be scaled more than the larger spin moment (cf. Fig. S3 [18]). In our XMCD experiments, the measured moments are scaled individually according to separate Langevin fits of spin and orbital moments. In Stern-Gerlach experiments, however, such an individual scaling is not possible.

The data of Payne *et al.* [16] have been measured with a considerably lower magnetic field (0.2–0.3 T). Under these conditions, spin and orbital moments are most likely coupled by spin-orbit interaction and interact as a total moment with the external magnetic field. In this case, Langevin scaling of the total moment becomes appropriate. This might explain the rather good agreement of the temperature-scaled data of Payne *et al.* [16] with the sum of m_S and m_L as determined from our high-field XMCD measurements in which the uncoupled moments are scaled separately before summing up.

In summary, the present data demonstrate the importance of quantifying spin and orbital moments as a function of temperature in order to analyze the intrinsic magnetic properties of free ferromagnetic particles. A clear Langevin-type temperature dependence has been established for small Co clusters revealing a different temperature scaling of spin and orbital moments under high magnetic field conditions. The data demonstrate that the intrinsic orbital moments of small Co clusters are strongly

enlarged by a factor of 4–6 in comparison to the bulk. The decomposition of the total moments into spin and orbital moments and their different temperature dependence might help to clarify diverging results of former Stern-Gerlach experiments. The analysis of spin and orbital magnetic moments of free clusters bears high potential for future investigation of application-relevant magnetic storage particles such as magnetic building block clusters, molecular magnets, and magnetic biomolecules.

This work has been supported by the DFG (Nie325/10-1). We are grateful to K. Fauth (University of Würzburg), T. Lau (Helmholtz-Zentrum Berlin), and W. Wurth (University of Hamburg) as well as P. Bechthold and S. Bluegel (Forschungszentrum Jülich) for valuable discussions. We also thank P. Hofmann (Brandenburg University of Technology, Cottbus) for assisting at the UE52 beam line.

-
- [1] G. Schütz, W. Wagner, W. Wilhelm, P. Kienle, R. Zeller, R. Frahm, and G. Materlik, *Phys. Rev. Lett.* **58**, 737 (1987).
- [2] J. Stöhr, *J. Electron Spectrosc. Relat. Phenom.* **75**, 253 (1995).
- [3] M. L. Billas, A. Chatelain, and W. A. de Heer, *Science* **265**, 1682 (1994).
- [4] S. E. Apsel, J. W. Emmert, J. Deng, and L. A. Bloomfield, *Phys. Rev. Lett.* **76**, 1441 (1996).
- [5] M. B. Knickelbein, *J. Chem. Phys.* **125**, 044308 (2006).
- [6] R. Guirado-Lopez, J. Dorantes-Davila, and G. Pastor, *Phys. Rev. Lett.* **90**, 226402 (2003).
- [7] B. Nonas, I. Cabria, R. Zeller, P. Dederichs, T. Huhne, and H. Ebert, *Phys. Rev. Lett.* **86**, 2146 (2001).
- [8] S. Datta, M. Kabir, S. Ganguly, B. Sanyal, T. Saha-Dasgupta, and A. Mookerjee, *Phys. Rev. B* **76**, 014429 (2007).
- [9] P. Gambardella, A. Dallmeyer, K. Maiti, M. Malagoli, W. Eberhardt, K. Kern, and C. Carbone, *Nature (London)* **416**, 301 (2002).
- [10] J. T. Lau, A. Föhlisch, R. Nietubyc, M. Reif, and W. Wurth, *Phys. Rev. Lett.* **89**, 057201 (2002).
- [11] J. Bansmann, A. Kleibert, M. Getzlaff, A. Rodriguez, F. Nolting, C. Boeglin, and K. Meiwes-Broer, *Phys. Status Solidi B* **247**, 1152 (2010).
- [12] K. Fauth, M. Heßler, D. Batchelor, and G. Schütz, *Surf. Sci.* **529**, 397 (2003).
- [13] H. Dürr, S. Dhesi, E. Dudzik, D. Knabben, G. van der Laan, J. Goedkop, and F. Hillebrecht, *Phys. Rev. B* **59**, R701 (1999).
- [14] H. Brune and P. Gambardella, *Surf. Sci.* **603**, 1812 (2009).
- [15] X. Xu, S. Yin, R. Moro, and W. de Heer, *Phys. Rev. Lett.* **95**, 237209 (2005).
- [16] F. W. Payne, W. Jiang, J. W. Emmert, J. Deng, and L. A. Bloomfield, *Phys. Rev. B* **75**, 094431 (2007).
- [17] S. Peredkov, A. Savci, S. Peters, M. Neeb, W. Eberhardt, H. Kampschulte, J. Meyer, M. Tombers, B. Hofferberth, F. Menges, and G. Niedner-Schatteburg, *J. Electron Spectrosc. Relat. Phenom.* **184**, 113 (2011).
- [18] See Supplemental Material at <http://link.aps.org/supplemental/10.1103/PhysRevLett.107.233401> for a description of the experimental setup (S1), a table showing measured and scaled magnetic moments (S2), and a graph showing scaling factors of magnetic moments as a function of temperature and different magnetic field strengths.
- [19] B. Thole, P. Carra, F. Sette, and G. van der Laan, *Phys. Rev. Lett.* **68**, 1943 (1992).
- [20] P. Carra, B. Thole, M. Altarelli, and X. Wang, *Phys. Rev. Lett.* **70**, 694 (1993).
- [21] C. Chen, Y. Idzerda, H.-J. Lin, N. Smith, G. Meigs, E. Chaban, G. Ho, E. Pellegrin, and F. Sette, *Phys. Rev. Lett.* **75**, 152 (1995).
- [22] By using the Langevin formalism, the intrinsic moments of superparamagnetic particles can be received from the measured moments.
- [23] G. Gutsev, S. Khanna, and P. Jena, *Chem. Phys. Lett.* **345**, 481 (2001).
- [24] O. Sipr, J. Minar, and H. Ebert, *Europhys. Lett.* **87**, 67007 (2009).
- [25] J. Stöhr and R. Nakajima, *IBM J. Res. Dev.* **42**, 73 (1998).
- [26] J. Stöhr and H. König, *Phys. Rev. Lett.* **75**, 3748 (1995).
- [27] R. Wu and A. Freeman, *Phys. Rev. Lett.* **73**, 1994 (1994).
- [28] S. Palutke, I. Baev, M. Martins, W. Wurth, J. Meyer, M. Tombers, G. Niedner-Schatteburg, S. Peredkov, M. Neeb, and W. Eberhardt (to be published).
- [29] S. Khanna and S. Linderoth, *Phys. Rev. Lett.* **67**, 742 (1991).
- [30] J. Bucher, D. Douglass, and L. Bloomfield, *Phys. Rev. Lett.* **66**, 3052 (1991).
- [31] B. Reddy, S. Nayak, S. Khanna, B. Rao, and P. Jena, *J. Phys. Chem. A* **102**, 1748 (1998).
- [32] J. Stöhr, *J. Magn. Magn. Mater.* **200**, 470 (1999).
- [33] G. Daalderop, P. Kelly, and M. Schuurmanns, *Phys. Rev. B* **50**, 9989 (1994).
- [34] M. Knickelbein, *J. Chem. Phys.* **121**, 5281 (2004).
- [35] P. Gambardella, S. Rusponi, M. Veronese, S. Dhesi, C. Grazioli, A. Dallmeyer, I. Cabria, R. Zeller, P. Dederichs, K. Kern, C. Carbone, and H. Brune, *Science* **300**, 1130 (2003).
- [36] H. Wang, Y. Khait, and M. Hoffmann, *Mol. Phys.* **103**, 263 (2005).
- [37] F. Furche and J. Perdew, *J. Chem. Phys.* **124**, 044103 (2006).
- [38] D. Hales and P. Armentrout, *J. Cluster Sci.* **1**, 127 (1990).
- [39] We assume that the extra charge does not much alter the magnetic moments of the ionized clusters, as the single hole is just a small fraction of the total number of valence electrons for $N \geq 8$ atoms (≥ 72 electrons).